Int. J. Nano Dimens., 14 (1): 60-72, Winter 2023

ORIGINAL ARTICLE

Antibacterial activity of the Iron-Zinc Oxide nanoparticles synthesized via electric discharge method

Fereshteh Shahbazi[1], Reza Ahmadi[1,], Mohammad Noghani[1], Gholamreza Karimi[2]*

[1] *Department of Materials Science and Metallurgy, Imam Khomeini International University, Qazvin, Iran*
[2] *Department of Mining Engineering, Imam Khomeini International University, Qazvin, Iran*

Received 10 July 2022; revised 05 November 2022; accepted 15 November 2022; available online 21 November 2022

Abstract

Recently, with the increase in diseases caused by bacterial and viral infections, the need for antibacterial agents has widely increased. On the other hand, with the development of drug resistance to organic groups of antibiotics, new antibiotics have attracted the attention of researchers because new methods are needed to reduce the activity of bacteria. Nanotechnology is increasingly being used for medical applications and is useful as an approach to kill or reduce the activity of various microorganisms. Metal oxides are considered for medical applications, especially as antibacterial agents, due to their potential advantages and suitable nanoscale properties. In this study, the electric discharge method was employed for the preparation of the iron oxide nanoparticles (IONPs) and iron-zinc oxide nanoparticles (IZONPs). As the IONPs and zinc oxide nanoparticles (ZONPs) attack various gram-positive and gram-negative bacteria by different mechanisms, it seems that the simultaneous use of these oxides can effectively kill various bacteria in outdoor and indoor media. The synthesized nanoparticles were characterized via XRD, UV-Visible, FE-SEM, EDS, HR-TEM, and TEM techniques. The obtained results showed that the IZONPs with mean particles size between 11 and 33 nanometers have successfully been synthesized in various experimental conditions. Also, the antibacterial properties of these nanoparticles were evaluated and the particles showed antibacterial properties against both gram-positive and gram-negative bacteria.

Keywords: *Antibacterial; B. Subtilis; E. Coli; Fe_3O_4 Nanoparticles; ZnO Nanoparticles.*

How to cite this article

Shahbazi F., Ahmadi R., NoghaniM., Karimi G.h. Antibacterial activity of the Iron-Zinc Oxide nanoparticles synthesized via electric discharge method. Int. J. Nano Dimens., 2023; 14(1): 60-72.

INTRODUCTION

Antibacterial agents play an important role in various industries such as medicine, textile industry, food industry and also for disinfecting water [1-3]. Recently, metal NPs have shown unique properties in different industries and medical processes. High specific surface area and the uniform distribution of NPs has made them suitable for various applications [4]. Antibacterial metal nanoparticles have an inhibitory effect on growth of both gram-positive and gram-negative bacteria and kill them through various proposed mechanisms such as Reactive Oxygen Species (ROS), membrane processes and the entry of nanoparticles into the bacteria, the release of ionic metals or direct destruction of bacterial membranes [5-7]. Among the various NPs, IONPs, ZONPs and IZONPs have attracted the attention of researchers due to their high antibacterial properties and cost-effectiveness [8]. The ZONPs show strong antibacterial effects through various mechanisms such as photocatalytic bacterial degradation, formation of ROS species, release of antimicrobial ions and electrostatic interactions [9]. Also, the complex metal oxide nanostructurs such as Zn-Fe-Mn oxide nanomaterials have shown excellent antibacterial effects due to the different mechanisms of each oxide [10]. There are several cost-effective methods to synthesis the ZONPs,

* Corresponding Author Email: re.ahmadi@eng.ikiu.ac.ir

Table 1. The chemical composition of the used ST37 wires.

Element	C	Si	Mn	P	S	Cr	Ni	Fe
Wt%	0.11	0.03	0.56	0.007	0.005	0.07	0.03	Balance

IONPs and IZONPs; Such as sol-gel [9], Thermal Decomposition [11], chemical precipitation [12, 13], green synthesis methods [14-16], electrochemical [17], electrical arc discharge [18] and electrical wire explosion [19]. The electrical discharge method is performed in a liquid or gaseous medium, which has been considered by researchers because of its cost-effectiveness and eco-friendly compared to other methods [4, 20]. Metallic wire evaporates by high voltage and current intensity. The NPs are then nucleated by cooling in a liquid or gaseous medium. With this method, it is possible to produce high purity metal NPs, oxide nanoparticles as well as composite NPs [4, 18, 19]. The properties and nature of the nanoparticles synthesized by electrical discharge method depend on factors such as synthesis environment, wire diameter, nature of wire metal, geometric shape of wire, parameters related to electric current and applied voltage and other things [21, 22]. Environmental parameters such as pressure, pH, surfactant addition and temperature greatly influence the properties of the synthesized NPs [23, 24].

In this study, IONPs and IZONPs were synthesized at constant pH, in different current intensities and different wire diameters, by electric discharge in a liquid medium [25]. Firstly, IONPs were synthesized by changing the diameter and current intensity parameters. Next, IZONPs were synthesized in optimized current intensity and diameter [26]. The synthesized NPs were characterized by XRD, UV-VISIBLE, FE-SEM, TEM and HRTEM techniques. The antibacterial properties of NPs against two types of gram-positive and gram-negative bacteria were investigated by wet and dry methods.

MATERIALS AND METHODS

Synthesis of oxide NPs

0.2 mm ST37 wires were used as the anode and cathode electrodes in the electrical discharge system and the arc discharge was conducted in a plastic container which containing distilled water with pH=7. The applied current was 300, 400 and 500 amps. The ST37 wire chemical composition is presented in table 1. According to the obtained initial results, the current intensity of 500 amps was selected as the optimal current. Then wires with 0.3, 0.4 and 0.5 mm size in diameter were employed through the arc discharge under 500 amps current

Table 2. Specifications and characterization results of synthesized samples prepared via electric discharge method in distilled water with pH=7.

Sample code	Electrodes	Current Intensity (A)	Diameter (mm)	Fe_3O_4 percentage (%)	Fe percentage (%)	ZnO percentage (%)	$ZnFe_2O_4$ percentage (%)	The average crystallite size (nm) (XRD)	The average particle size (nm) (SEM)
S01	St37 Wire	300	0.2	89	11	_	_	17	35.85
S02	St37 Wire	400	0.2	90	10	_	_	10.45	20.25
S03	St37 Wire	500	0.2	93	7	_	_	8	10.3
S04	St37 Wire	500	0.3	91	9	_	_	27.24	17.7
S05	St37 Wire	500	0.4	88	12	_	_	29.32	26.25
S06	St37 Wire	500	0.5	85	15	_	_	30.45	35.5
S07	Zn Coated St37 Wire	500	0.2	_	_	65	35	18.46	30.9

intensity. In the next step, the ST37 wires were dipped into molten Zn. The Zn-coated ST37 wires were employed as the anode and cathode using an 80 V DC power supply. With starting electrical discharge process, the atoms evaporate and then cool rapidly in the water to form oxide NPs. The synthesis conditions are listed in table 2.

Characterization of oxide NPs

The synthesized samples were characterized via X-ray Diffractometer (XRD, model PANalytical with Cu K_α radiation of1.54060 Å ,voltage 40 kV, current intensity 40 mA and step size 0.026˚, The range of 2theta was 5 - 80˚C), UV-Vis spectroscopy (using UV-1800 spectrophotometer), Field Emission Scanning Electron Microscopy (FESEM, Model MIRA3TESCAN-XMU) equipped with Energy Dispersive Spectroscope (EDS), Transmission Electron Microscopy (TEM model Leo 912 AB) and High-Resolution Transmission Electron Microscopy (HR-TEM FEI TECNAI F20) for structural and morphological analysis.

Antibacterial assay

To determine the effectiveness of nanoparticles as antibacterial agents, several experimental techniques are used that measure bacterial survival after exposure to nanoparticles. In 2006, the Institute for Clinical and Laboratory Standards (CLSI) published a document entitled "Analysis and Presentation of Antimicrobial Sensitivity Test Data" which sets out the standards required for antibacterial testing. Gram-positive and gram-negative bacteria may react differently to antibacterial nanoparticles. Therefore, studies often include at least one gram-positive species and one gram-negative species to determine antibiotic efficacy [27, 28].

Specifications of culture medium and bacteria

The LB broth and agar powders (QUELAB Germany) were used to prepare liquid and solid culture media for bacteria, respectively. Müller-Hinton Broth (MHB) culture medium (QUELAB Germany) was also used to evaluate the MIC. The studied bacteria were gram-negative *Escherichia coli* MHD5 and gram-positive *Bacillus subtilis*.

Growth curve analysis

The antibacterial evaluation of the prepared nanoparticles was first performed by determining the optical density (OD). To prepare the liquid culture medium, 1.75 g of LB powder was poured into 50 ml of distilled water in an Erlenmeyer flask and placed in an autoclave at 121.5 ° C and 1.5 atmospheres for 20 minutes. Both bacteria were then separately inoculated into culture medium and placed in an incubator shaker at 37 ° C to suspend the bacterium equivalent to the 0.5 McFarland standard. Then, by adding equal amounts of bacterial suspension and adding different amounts of nanoparticles to the liquid culture medium, 4 samples with various nanoparticle concentrations of 156, 312, 625 and 1250 ppm were prepared. The samples were then placed in an incubator-shaker at 37 ° C and after each 2-hour period, the optical density at 600 nm was measured by the Spectro UV-VIS UVD-3200. The control samples were not exposed to nanoparticles.

Minimum Inhibitory Concentration (MIC)

To ensure the obtained antibacterial results, the

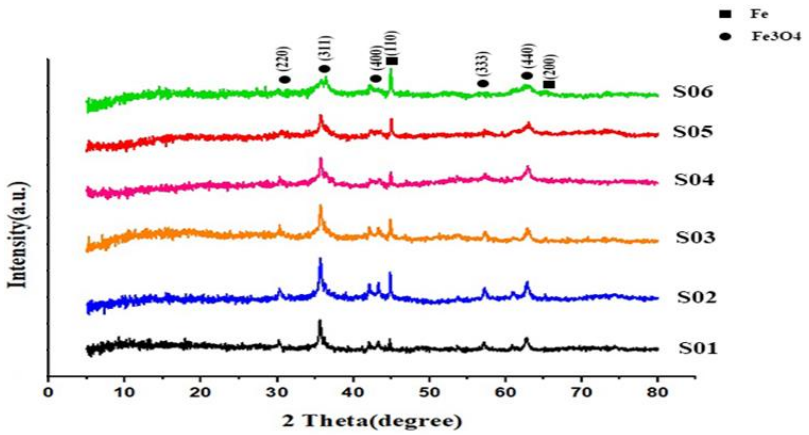

Fig. 1. XRD pattern of the IONPs prepared by the electric discharge in liquid.

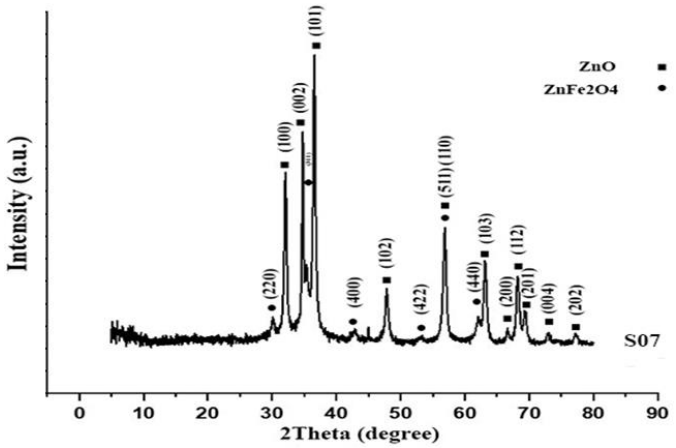

Fig. 2. XRD pattern of the IZONPs prepared by the electric discharge in liquid.

antibacterial effects of the IONPs and IZONPs were evaluated using standard dilution method (CLSI M07-A8).

To prepare the liquid culture medium, 1.05 g of MHB powder per 50 ml was poured into distilled water in an Erlenmeyer flask and placed in an autoclave at 121.5 ° C and 1.5 atmospheres for 20 minutes. Each bacterium was then inoculated into the culture medium separately to obtain a bacterial suspension equivalent to the half McFarland standard. 100 µl of freshly prepared culture medium was poured into each 96-well plate well. Then 100 µl of nanoparticle suspension was poured into the first row wells and dilution was performed from top to bottom in all wells. Then 100 µl of the bacterial suspension was added to each cell. Two replicates were placed for each sample. One column was placed for positive control and one column for negative control. Also, one column for each sample was placed as a control sample that contained only culture medium and nanoparticles. The plates were covered with parafilm and left for 24 hours in the incubator-shaker at 37 ° C. After incubation, 40 µl of tetrazolium salt (MTT) with a concentration of 0.2 mg/ml was added to each well and placed at room temperature for 15 minutes. The growth of the bacteria is determined with purple or pink appearance. If the growth of bacteria is stopped, the corresponding well will appear colorless which the concentration of that well is considered as the amount of MIC. Finally, the plate was examined with an ELISA reader with a wavelength of 600 nm. All steps related to this test were performed under a microbial hood.

RESULTS AND DISCUSSION

NPs characterizations

X-ray diffraction

The XRD patterns of the prepared IONPs are shown in fig. 1. As seen, the XRD patterns reveal the characteristic diffraction peaks of cubic Fe_3O_4 (ICDD no. 01-088-0315) and cubic Fe phases (ICDD no. 01-087-0722), respectively [8, 29]. The XRD pattern related to the S07 sample (table 2) is presented in fig. 2 which exhibit diffraction peaks of hexagonal ZnO (ICDD no. 01-079-0205) and cubic $ZnFe_2O_4$ phases (ICDD no. 01-089-1010), respectively [1, 30, 31]. In the case of the IONPs,

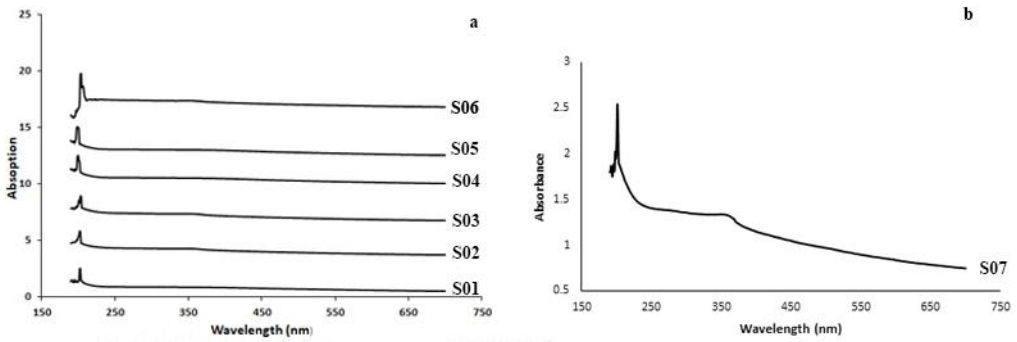

Fig. 3. Uv-Vis spectra of a) IONPs and b) IZONPs.

as the free Oxygen atoms are available only for the surface atoms of the wire, not for the whole atoms, so the atoms located in the center of the wire will not react with the Oxygen atoms and the peaks related to the Fe and Fe_3O_4 phases are both present in the XRD pattern. In the case of S07 sample, the Zinc layer is located only in the surface part of wire, so the free Oxygen atoms are completely available for the all of the Zn atoms and due to the high chemical reactivity of the Zn atoms, Zinc will present completely in the Oxide form. So, there are not any peaks related to the Zn phase in the XRD pattern (fig. 2). The weight percentage of each phase was calculated using Rietveld method. The results are shown in Table 2. It is clear that increasing the electric current and decreasing the diameter has increased the oxide phase. Also, the percentage of metal phase in the sample with a larger diameter is higher than other samples. It is due to this fact that the ratio of the surface atoms to the whole number of atoms is greater for the thinner wire, so the free Oxygen atoms are more available for the Iron atoms and the percentage of Oxide phase increases with the decrement of wire diameter. The average crystallite sizes of the all samples were calculated using Scherrer's formula and presented in Table 2.

Increasing the electric current intensity increases the driving force needed to create finer nuclei of nanoparticles, the result is nanoparticles with smaller grain sizes. On the other hand,

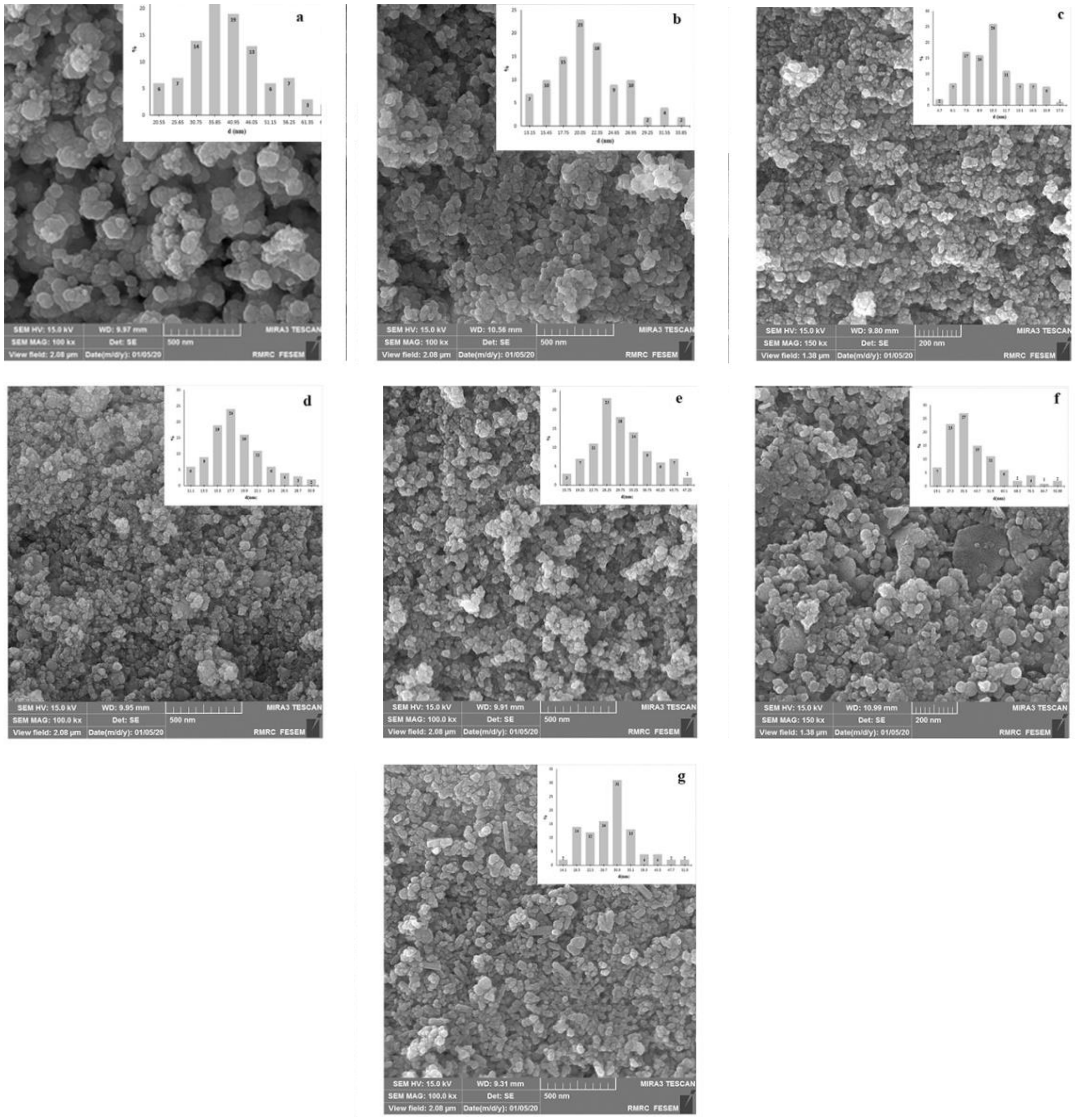

Fig. 4. FESEM images of samples: a)S01, b)S02, c)S03, d)S04, e)S05, f)S06 and g)S07.

nanoparticles can form and grow both directly from plasma and from existing solid nuclei. High current intensity and high cooling rate probably lead to the formation of nanoparticles with smaller granulation [26, 32, 33].

As the wire diameter decreases and the resulting particle size decreases, the percentage of oxide phase increases. Oxidation of metal nanoparticles depends on the particle size too. Oxidation is a chemical reaction that takes place on the surface; So in order to continue the reaction, more levels must be provided for the reaction. The smaller the particle size, the greater the amount of surface atoms; therefore, as the diameter decreases, the percentage of surface atoms that have access to oxygen due to water evaporation increases, so as the wire diameter decreases and the particle size decreases, the percentage of oxide phase increases [34- 36]. As the oxide phase increases, the antibacterial property intensifies through the ROS mechanism.

UV-Visible

The UV-Visible spectra of IONPs and IZONPs are shown in figs. 3a and 3b, respectively. As seen, the IONPs had an absorption peak in the range of 200 nm. The particle size and surface area of nanoparticles affect the absorption peak intensity. IZONPs had two absorption peaks in the range of 300 and 350nm which are related to ZnO and $ZnFe_2O_4$, respectively [37, 38].

Field emission scanning electron microscopy

The SEM images of IONPs and IZONPs are shown in Figs. 4a, 4b, 4c, 4d, 4e, 4f and 4g. It can be clearly seen that the IONPs are completely uniform and spherical in shape. However, in the image related to the sample S07, particles in rod shaped and needle-shaped are seen, which is due to the presence of IZONPs. FESEM images are taken from a powder sample, and also because of the magnetic nature of IONPs, the aggregation of nanoparticles and the formation of clusters has been done to a large extent [20, 25, 39]. The average particle size of the samples is given in Table 2.

In the liquid media, in contrast to gaseous media, the size of nanoparticles decreases with increasing the current intensity. As the current intensity increases, the energy input to the wires increases, and fine-grained melt buds are formed during electrical discharge, and due the high cooling rate of these fine particles, nanoparticles with smaller size are produced [25, 34, 40].

TEM and HR-TEM

Figs. 5a, 5b, 5c, 5d, 5e and 5f show the TEM images of the synthesized samples. As seen, the synthesized IONPs have a spherical and uniform

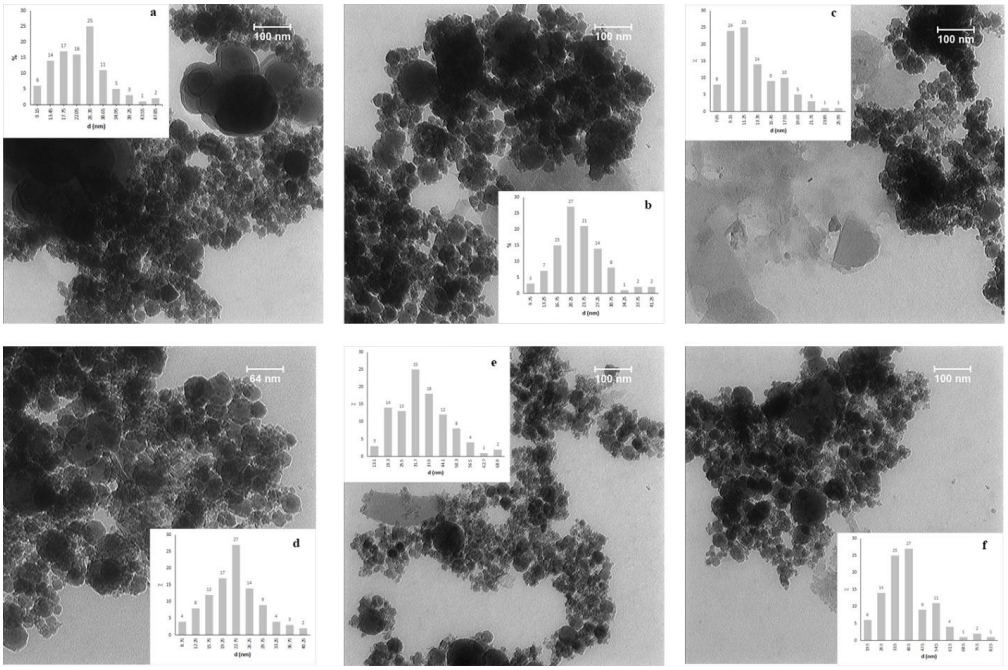

Fig. 5. TEM images of samples: a) S01, b) S02, c) S03, d) S04, e) S05 and f) S06.

morphology. With increasing current intensity from 300 amps to 500 amps, the average particle size has decreased from 26.50 nm to 11.25 nm. Also, by reducing the wire diameter from 0.5 mm to 0.2 mm, the average particle size has decreased from 33.50 nm to 11.25 nm. In addition, the images show the core-shell structure. Other researchers have reported the similar results in which the core and shell contains the iron and iron oxide phases, respectively [41, 42].

Figs. 6a and 6b show the TEM images of IZONPs. The IZONPs with a rod structure are seen in these images. The average particle size is in the range of 20 nanometers. Also Figs. 6c and d present the SAED pattern and HR-TEM images, respectively. Some spots have been determined and attributed to the metal oxide crystallographic planes and indexed in SAED pattern of fig. 6c using the equation rd = Lλ in which r and d are the ring radius and the distance between adjacent lattice planes and Lλ is the TEM camera constant. As seen, the specified planes are in good coincidences with the XRD data (fig. 2).

NPs antibacterial activity

Growth curve analysis

Figs. 7 and 8 reveal the antibacterial activity of iron nanoparticles against both bacteria. The best result is obtained in the S03 and S07 samples, which have the lower average particle size (according to SEM and XRD images).

In each chart, bacterial growth is reduced or completely inhibited by increasing the concentration. This phenomenon can be exacerbated by the interaction between bacteria and nanoparticles and thus the activation of antibacterial mechanisms. The effective mechanism for antibacterial effect of the IONPs is the ROS production process as well as the reaction of Fe^{2+} with oxygen to produce hydrogen peroxide. Eventually, H_2O_2 reacts with iron through the Fenton process to produce hydroxyl radicals that damage biological molecules [1, 30, 43].

In the case of sampleS06, it is clear that it has little effect on inhibiting bacterial growth due to the high presence of large nanoparticles (according to the SEM and XRD results) as well as the low percentage

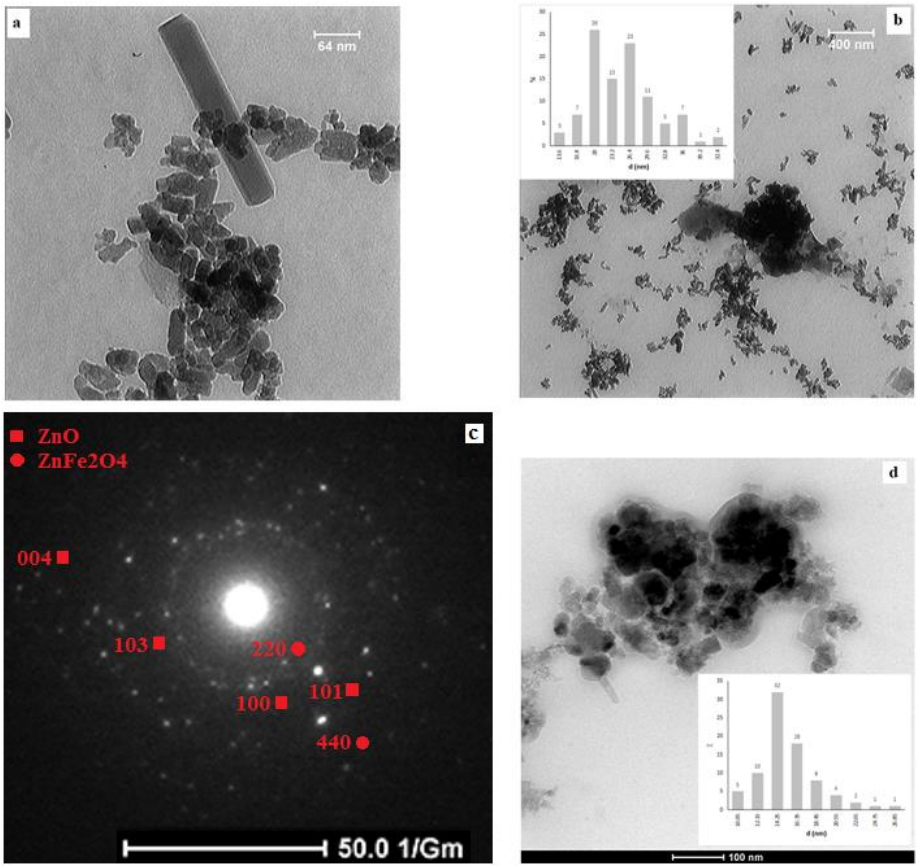

Fig. 6. a and b) TEM images of IZONPs, c) SAED pattern, d)HRTEM image of IZONPs.

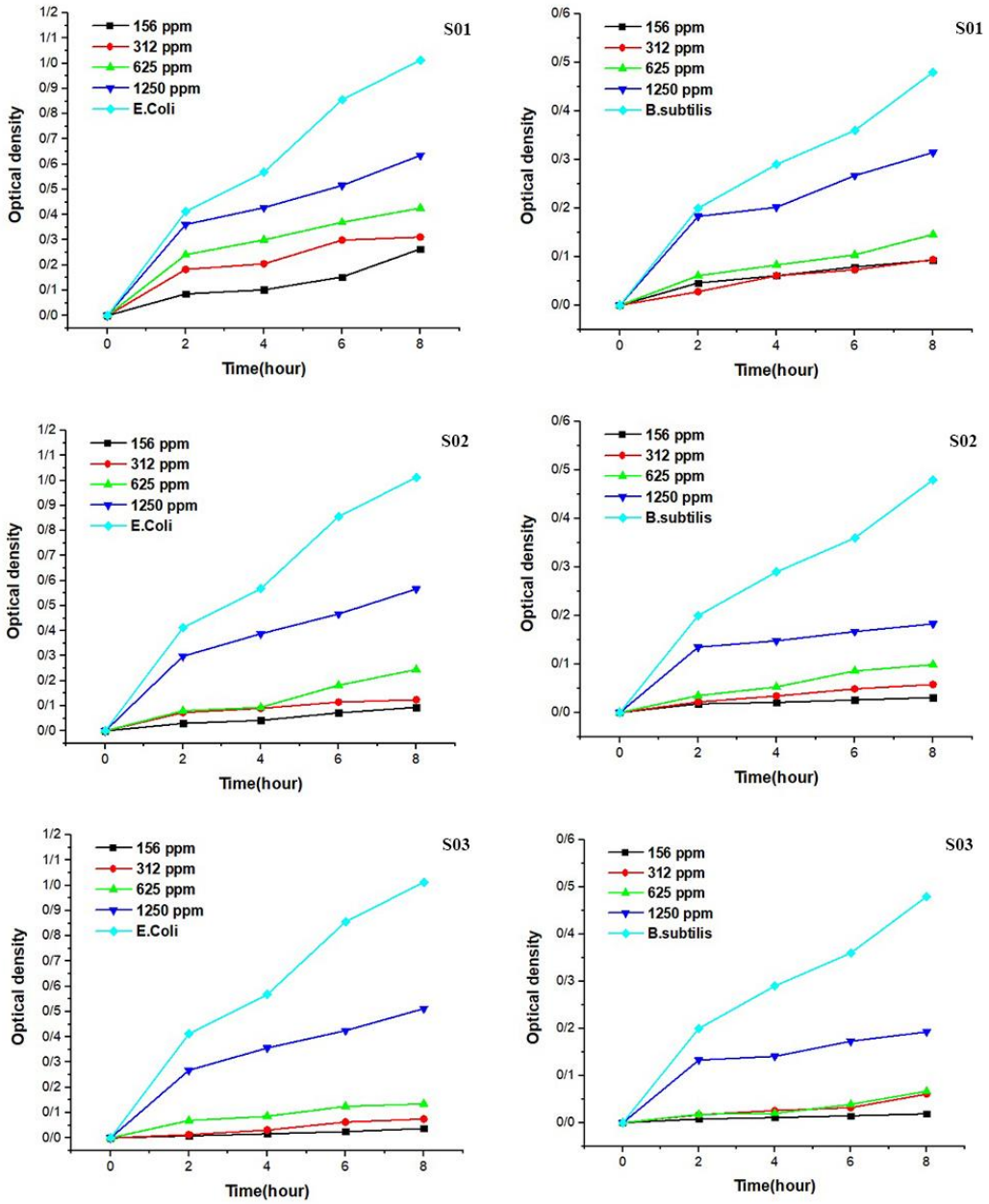

Fig. 7. Bacterial growth curve in the presence of synthesized nanoparticles.

of Fe_3O_4 in this sample. Researches has shown that the antibacterial effect of Fe_3O_4 is greater than other iron compounds due to its greater oxygen supply as a good source for oxidative stress reactions [43, 44].

The S07 sample showed high antibacterial properties compared to both bacteria. These results are due to the synergistic effect of the simultaneously presence of the Iron and Zinc Oxides and thus activating more antibacterial mechanisms. The mechanism related to the IONPs is the electrostatic interaction between nanoparticles and bacteria as well as the production of reactive oxygen species. The effective mechanisms for IZONPs can be expressed as electrostatic interaction between nanoparticles and bacteria, production of reactive oxygen species and ion release [4, 43, 44]. The obtained results are in good coincidence with other similar reports that show the effective antibacterial behavior of the Zn oxide and Fe-Zn-Mn oxides nanomaterials [9, 10].

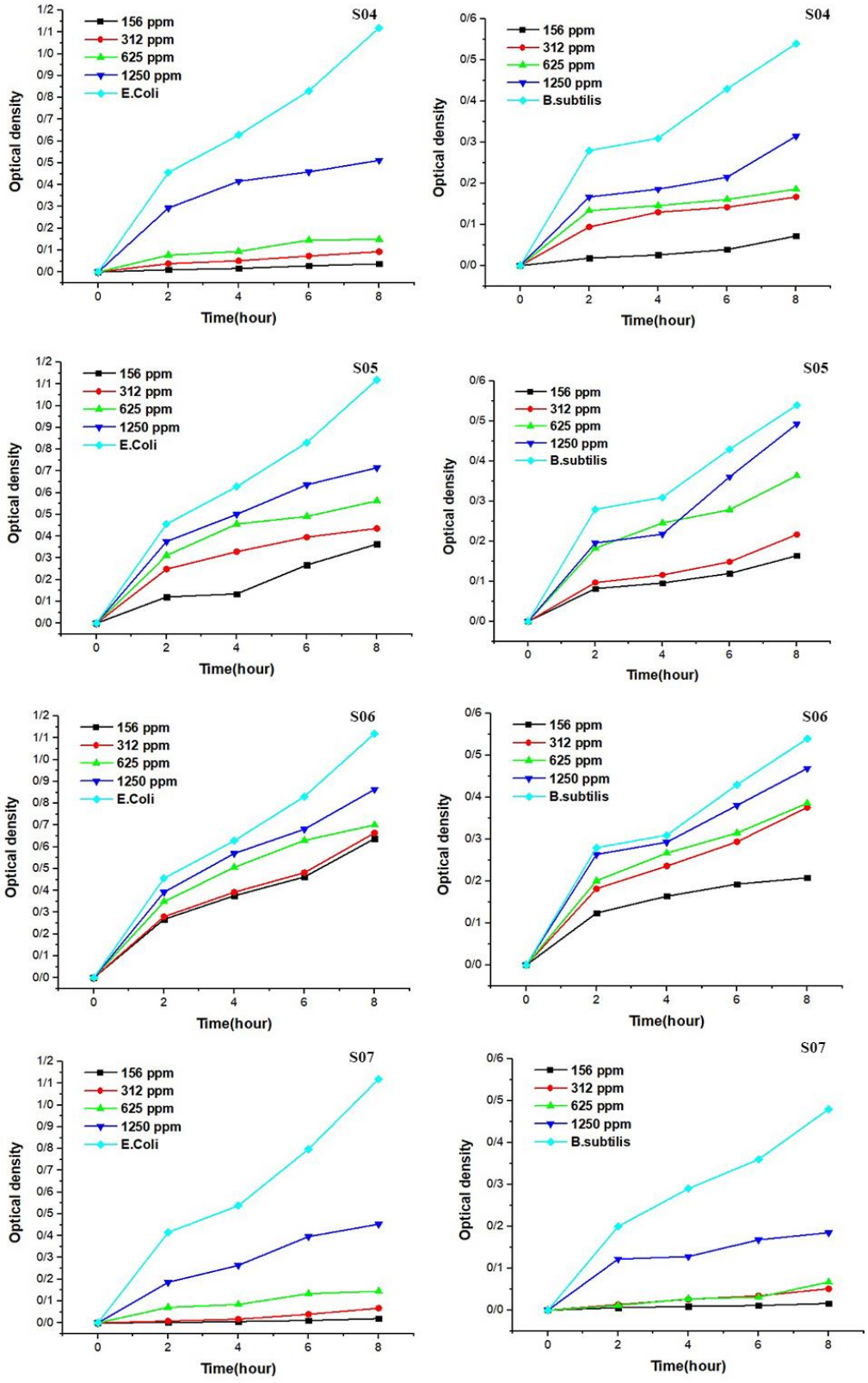

Fig. 8. Bacterial growth curves in the presence of synthesized nanoparticles.

Table 3. The result of MIC method for *E. Coli*.

Concentration(µg/ml)	S01	S02	S03	S04	S05	S06	S07	*E.Coli*
10000	-	-	-	-	-	0.0125	-	1.42
5000	-	-	-	-	-	0.03	-	1.491
2500	-	-	-	-	0.064	0.132	-	1.524
1250	-	-	-	-	0.1335	0.223	-	1.463
625	0.119	0.1425	0.05	0.1895	0.2625	0.406	-	1.403
312.5	0.1835	0.26	0.1245	0.2425	0.3455	0.601	0.0015	1.515
156.25	0.2245	0.3975	0.1685	0.357	0.4265	0.8875	0.102	1.468
78.125	0.3335	0.434	0.223	0.432	0.725	1.13	0.175	1.526

Minimum Inhibitory Concentration (MIC)

The results of the MIC method are presented in Tables 3 and 4. As seen, the S07 sample showed the best performance and the bacterial growth was completely stopped at concentrations higher than 312.5 µg/ml.

Simultaneous activation of antibacterial mechanisms of IONPs and IZONPs has created a synergistic effect in stopping the growth of bacteria. In the case of sample S06, even at the highest concentration, despite the positive effect, but complete cessation of growth is not seen. The large size of the nanoparticles has reduced the possibility of penetration into the bacterial cell and as a result this sample is less effective [5, 43, 45].

Figs. 9a and 9b show the antibacterial effect of nanoparticles against *E.Coli* and *B.Subtilis* bacteria by MIC method, respectively. According to these diagrams, with increasing current intensity at constant wire diameter, the antibacterial effect is improved and also by decreasing the wire diameter at constant current, the antibacterial activity of the samples is increased. Finally, based on the results obtained in the MIC method the bacterial strain of *E.Coli* is more sensitive than *B.Subtilis* [1, 46, 47].

CONCLUSIONS

In this study, IONPs and IZONPs were successfully synthesized by electric discharge method by controlling the parameters of electric current and wire diameter. The prepared samples were microstructurally analyzed by XRD, FESEM,

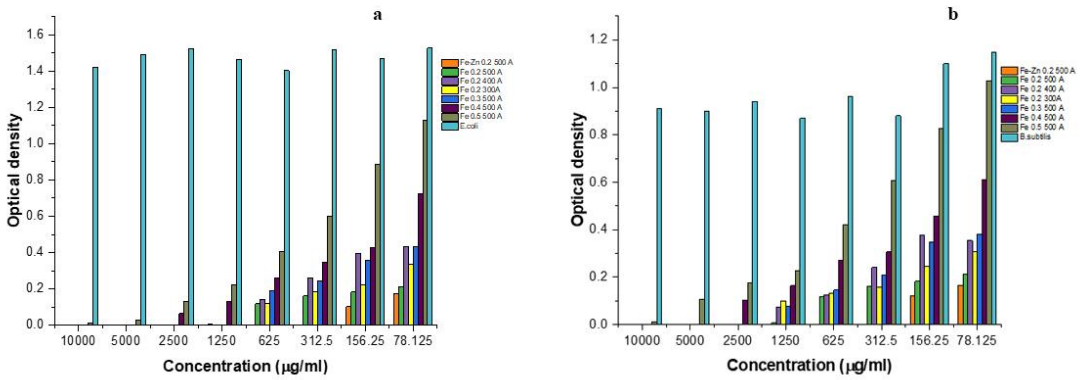

Fig. 9. Graphical results of antibacterial test by MIC method for a) *E.Coli*, b) *B.subtilis*.

Table 4. The result of MIC method for *B. Subtilis*.

Concentration(µg/ml)	S01	S02	S03	S04	S05	S06	S07	*B.Subtilis*
10000	-	-	-	-	-	0.0125	-	0.91
5000	-	-	-	-	-	0.1065	-	0.9
2500	-	-	-	-	0.1015	0.1745	-	0.94
1250	0.099	0.072	0.006	0.0765	0.164	0.228	-	0.87
625	0.131	0.1255	0.1185	0.1455	0.269	0.421	-	0.96
312.5	0.157	0.24	0.1625	0.208	0.306	0.606	-	0.88
156.25	0.2435	0.3765	0.1825	0.348	0.4575	0.825	0.1205	1.1
78.125	0.309	0.354	0.2125	0.381	0.6125	1.029	0.1645	1.15

UV-VISIBLE, TEM and HRTEM. The results showed that reducing the wire diameter and increasing the current have a positive effect on reducing the size of nanoparticles and also affect the metal oxide percentage. The effect of wire thickness on the metal oxide percentage was not studied before. Growth curve and MIC methods were used to evaluate the antibacterial properties of nanoparticles against gram-positive and gram-negative bacteria. Both bacteria showed sensitivity to nanoparticles. The antibacterial activity increased with decreasing the particles size and increasing the percentage of the oxide phase. Also, increasing the presence of Zinc Oxide had a positive effect on the antibacterial activity.

DECLARATION STATEMENT

The authors declare that they have no conflict of interest.

REFERENCES

1. Bhushan M., Kumar Y., Latha P., Vismanath A., (2018), Facile synthesis of Fe/Zn oxide nanocomposites and study of their structural, magnetic, thermal, antibacterial and cytotoxic properties. *Mater. Chem. Phys.* 209: 233-248.
2. Lewis K., (2013), Platforms for antibiotic discovery. *Nat. Rev. Drug Discov*. 12: 371-387.
3. Aminov R. I., (2009), The role of antibiotics and antibiotic resistance in nature. *Environ. Microbiol.* 11: 2970-2988.
4. Shahriyari F., Yarali D., Ahmadi R., Shabir H., Wei W., (2020), Synthesis and characterization of Cu-Sn oxides nanoparticles via wire explosion method with surfactants, evaluation of in-vitro cytotoxic and antibacterial properties. *Adv. Powder Tech.* 31: 2337-2347.
5. Mohammad J. H., Katharina M. F., Ashkarran A., Dorleta J., Idoia R., Teofilo R., Vahid S., Wolfgang J. P., Mahmoudi M., (2012), Antibacterial properties of nanoparticles. *Trends. Biotechnol.* 2012. 30: 499-511.
6. Slavica S., Sneha S., Franica H., Vidic J., (2016), Pure and multi metal oxide nanoparticles: Synthesis, antibacterial and cytotoxic properties. *J. Nanobiotechnol.* 14: 1-20.
7. Lemire J., Harrison J., Turner R., (2013), Antimicrobial activity of metals: Mechanisms, molecular targets and applications. *Nat. Rev. Microbiol.* 11: 371-384.
8. Zhang W., Shi X., Jing H., Zhang Y., Wu Z., Xian Y., (2012), Bacitracin-conjugated superparamagnetic iron oxide nanoparticles: Synthesis, characterization and antibacterial activity. *Chem. Physic. Chem.* 13: 3388-3396.
9. Buzuayehu A., Enyew A., Aschalew T., Ananda H. C., (2020), A review on enhancing the antibacterial activity of ZnO: Mechanisms and microscopic investigation. *Nanoscale Res. Lett.* 15: 1-19.
10. Buzuayehu A., Ananda H. C., Enyew A., Yeshaneh A., (2020), PVA assisted ZnO based mesoporous ternary metal oxides nanomaterials: Synthesis, optimization, and evaluation of antibacterial activity. *Mater. Res. Express.* 7: 1-13.
11. Lu A., Salabas E. L., Schüth F., (2007), Magnetic nanoparticles: Synthesis, protection, functionalization, and application. *Angew. Chem., Int. Ed.* 46: 1222-1244.
12. Nazari M., Ghasemi N., Madaah H., Mousavi M., (2014), Synthesis and characterization of maghemite nanopowders by chemical precipitation method. *J. Nanostructure Chem.* 4: 1-5.
13. Sadeghi B., Jamali M., Kia Sh., Amini Nia A., Ghafari S., (2010), Synthesis and characterization of Silver nanoparticles for antibacterial activity. *Int. J. Nano Dimens.* 1: 119-124.
14. Sadeghi B., Mohammadzadeh M., Babakhani B., (2015), Green synthesis of gold nanoparticles using Stevia

rebaudiana leaf extracts: Characterization and their stability. *J. Photoch. Photobio B.* 148: 101-1016.
15. Sadeghi B., Gholamhoseinpour F., (2015), A study on the stability and green synthesis of silver nanoparticles using *Ziziphora tenuior (Zt)* extract at room temperature. *Spectrochim. Acta A.* 134: 310-315.
16. Sintayehu T. G., Gemechis A. M., Ananda H. C., Endale T. M., Ravikumar C. R., Bedasa A. G., Fedlu K. S., (2022), Biogenic synthesis of magnetite (Fe_3O_4) nanoparticles using leaf extract of *Thymus schimperi* and application for removal of Chromium and Mercury ions from aqueous solution. *J. Nanomater.* 2022: 1-15.
17. Elrouby M., Abdel-Mawgoud A. M., El-Rahman R. A., (2017), Synthesis of Iron Oxides nanoparticles with very high saturation magnetization form TEA-Fe(III) complex via electrochemical deposition for supercapacitor applications. *J. Mol. Struct.* 1147: 84-95.
18. Kheradmand E., Delavari H., Poursalehi R., (2015), The effect of dissolved Oxygen in arc medium on crystal structure and optical properties of Iron based nanoparticles prepared via Dc arc discharge in water. *Proc. Mat. Sci.* 11: 695-699.
19. Song K., Kim W., Suh C., Shin D., Ko K., Ha K., (2013), Magnetic Iron Oxide nanoparticles prepared by electrical wire explosion for arsenic removal. *Powder Technol.* 246: 572-574.
20. Lerner M. I., Lozhkomoev A. S., Bakina O., (2016), Synthesis of Al nanoparticles and Al/AlN composite nanoparticles by electrical explosion of aluminum wires in argon and nitrogen. *Powder Technol.* 295: 307-314.
21. Raffi M., Saba M., Tariq M., Akhter J., Yavar W., Hasan M., (2010), Investigations into the antibacterial behavior of copper nanoparticles against *Escherichia coli. Ann. Microbiol.* 60: 75-80.
22. Sundaram R., Yamada T., Hata K., Sekiguchi A., (2017), Electrical performance of lightweight CNT-Cu composite wires impacted by surface and internal Cu spatial distribution. *Sci. Rep.* 7: 1-11.
23. Lee Y. S., Bora B., Yap S. L., Wong C. S., (2012), Effect of ambient air pressure on synthesis of copper and copper oxide nanoparticles by wire explosion process. *Curr. App. Phys.* 12: 199-203.
24. Park E., Park H. W., Lee J., (2015), Synthesis of hierarchical copper oxide composites prepared via electrical explosion of the wire in liquids method. *Colloid. Surf. A.* 482: 710-717.
25. Buazar F., Cheshmehkani A., Kassaee M. Z., (2012), Nanosteel synthesis via arc discharge: Media and current effects. *J. Iran. Chem. Soc.* 9: 151-156.
26. Kassaee M., Buazar F., Motamedi E., (2010), Effects of current on arc fabrication of Cu nanoparticles. *J. Nanomater.* 2010: 1-5.
27. Horvat R., (2010), Review of antibiogram preparation and susceptibility testing systems. *Hosp. Pharm.* 45: S6-S9.
28. Seil J. T., Webster T. J., (2012), Antimicrobial applications of nanotechnology: Methods and literature. *Int. J. Nanomed.* 7: 2767-2781.
29. Wasfi A. S., Humud H. R., Fadhil N. K., (2019), Synthesis of core-shell Fe_3O_4-Au nanoparticles by electrical exploding wire technique combined with laser pulse shooting. *Opt. Laser Technol.* 111: 720-726.
30. Farbod M., Movahed A., Kazeminezhad I., (2012), An investigation of structural phase transformation of monosize γ-Fe_2O_3 nanoparticles fabricated by arc discharge method. *Mater. Lett.* 89: 140-142.
31. Salamat S., Younesi H., Bahramifar N., (2017), Synthesis of magnetic core–shell Fe_3O_4@TiO_2 nanoparticles from electric arc furnace dust for photocatalytic degradation of steel mill wastewater. *RSC Adv.* 7: 19391-19405.
32. Taccogna F., (2015), Nucleation and growth of nanoparticles in a plasma by laser ablation in liquid. *J. Plasma Phys.* 81: 1-12.
33. Faraji M., Poursalehi R., Aliofkhazraei M., (2015), The effect of surfactant on colloidal stability, oxidation and optical properties of Aluminum nanoparticles prepared via Dc arc discharge in water. *Proc. Mat. Sci.* 11: 684-688.
34. Chernavskii P. A., Peskov N. V., Mugtasimov A. V., Lunin V. V., (2007), Oxidation of metal nanoparticles: Experiment and model. *Russ. J. Phys. Chem. B.* 1: 394-411.
35. Hedberg Y. S., Pradhan S., Cappellini F., Karlsson M.-E., Blomberg E., (2016), Electrochemical surface oxide characteristics of metal nanoparticles (Mn, Cu and Al) and the relation to toxicity. *Electrochim Acta.* 212: 360-371.
36. Ahmadi S., Fazilati M., Nazem H., Mousavi S. M., (2021), Green synthesis of magnetic nanoparticles using satureja hortensis essential ol toward superior antibacterial/fungal and anticancer performance. *BioMed. Res. Int.* 2021: 1-9.
37. Xu Q., Feng J., Li L., Xiao Q., Wang J., (2015), Hollow $ZnFe_2O_4$/TiO_2 composites: High-performance and recyclable visible-light photocatalyst. *J. Alloy. Compd.* 641: 110-118.
38. Vidhya K., Saravanan M., Bhoopathi G., Devarajan V. P., Subanya S., (2014), Structural and optical characterization of pure and starch-capped ZnO quantum dots and their photocatalytic activity. *Appl. Nanosci.* 5: 235-243.
39. Shabgard M. R., Najafabadi A. F., (2014), The influence of dielectric media on nano-structured tungsten carbide (WC) powder synthesized by electro-discharge process. *Adv. Powder Technol.* 25: 937-945.
40. Karakoti A. S., Munusamy P., Hostetler K., Kodali V., Kuchibhatla S., Orr G., Pounds J. G., Teeguarden J. G., Thrall B. D., Baer D. R., (2012), Preparation and characterization challenges to understanding environmental and biological impacts of nanoparticles. *Surf. Interface Anal.* 44: 882-889.
41. Predescu A., Matei E., Berbecaru A., Cristian P., Dragan C., Vidu R., Kuncser V., (2018), Synthesis and characterization of dextran-coated Iron Oxide nanoparticles. *Roy. Soc. Open Sci.* 5: 1-16.
42. Lari L., Steinhauer S., Lazarov V. K., (2020), In situ TEM oxidation study of Fe thin-film transformation to single-crystal magnetite nanoparticles. *J. Mater. Sci.* 55: 12897-12905.
43. Arakha M., Pal S., Devyani S., Tapan K., Bairaji C., Krishna P., Mallick B., Jha S., (2015), Antimicrobial activity of iron oxide nanoparticle upon modulation of nanoparticle-bacteria interface. *Sci. Rep.* 5: 1-14.
44. Yusof N. A. A., Zain N. M., Pauzi N., (2019), Synthesis of ZnO nanoparticles with chitosan as stabilizing agent and their antibacterial properties against Gram-positive and Gram-negative bacteria. *Int. J. Biol. Macromol.* 124: 1132-1136.
45. Rajabi S. K., Sohrabnezhad S., (2018), Fabrication and characteristic of Fe_3O_4@MOR@CuO core-shell for investigation antibacterial properties. *J. Fluorine Chem.* 206: 36-42.
46. Riaz M., Zia R., Saleemi F., Hussain T., (2018), In Vitro antibacterial activity of Ta_2O_5 doped glass-ceramics against pathogenic bacteria. *J. Alloy. Compd.* 764: 10-16.
47. Armijo L. M., Wawrzyniec S. J., Kopciuch M., Brandt Y.,

Rivera A., (2020), Antibacterial activity of iron oxide, iron nitride, and tobramycin conjugated nanoparticles against *Pseudomonas aeruginosa* biofilms. *J. Nanobiotechnol.* 18: 1-27.